

Design and fabrication of polymeric multimode power splitter with secondary asymmetric branches

Shu Li (李 书), Qiao Lin (林 巧), Liuhua Chen (陈柳华), and Xingkun Wu (吴兴坤)*

State Key Laboratory of Modern Optical Instrumentation, Department of Optical Engineering,
Zhejiang University, Hangzhou 310027, China

*Corresponding author: xingkunwu@zju.edu.cn

Received December 20, 2010; accepted March 15, 2011; posted online June 16, 2011

A novel design of multimode light power splitter is proposed and fabricated by using secondary asymmetric Y branches. An almost equally divided output among output terminals is obtained experimentally. Maskless laser direct writing technique is applied in the fabrication process to facilitate the formation of power splitters by ultraviolet curable polymer. The analysis of the performances of both four-port and eight-port devices shows that these two dividers obtain a power splitting uniformity of more than 95%.

OCIS codes: 130.3120, 130.5460, 220.4610.

doi: 10.3788/COL201109.081302.

Integrated optical devices have long been an interest to researchers for their potentials^[1–3]. These devices are generally divided into single-mode and multimode types. Single-mode components are commonly used in long-haul optical communication networks for their low loss characteristic, whereas in the case of short-ranged systems such as information transportation for all-optical board interconnection^[4], multimode counterparts are more advantageous. Local area network (LAN) communications and many other medical or industrial applications where multimode light sources suffice could use multimode devices.

As a key element in optical networks, single-mode power splitters in many formats have been studied^[5–7]. In addition, they have been used in many commercialized applications. However, in the case of multimode devices, their splitter structure has special requirements for achieving equal power splitting as there is uncertainty in power mode. A 1×2 multimode splitter was reported^[8] where a masked ion-exchange process was introduced and the device was long. However, complexity in mode distribution continues to be a main obstacle to high-port devices.

Lithography and ion exchange are two commonly used techniques for integrated device fabrication, requiring high-quality mask or mold. On the other hand, there have been efforts to simplify the design and fabrication process for integrated devices in an attempt to achieve high efficiency and cost reduction^[9,10]. This maskless method is called laser direct writing. Planar waveguide devices written this way have been reported as couplers, splitters, and even attenuators^[11–13]. They have the advantages of convenience and low fabrication cost. In this letter, a novel design of the multimode splitter structure is proposed and realized under the method of mask-free ultraviolet (UV) direct writing.

Y branch is an essential part in the construction of optical splitters. The Y branch in straight lines has been introduced in previous work^[14], but this type of structure sets a high fabrication requirement—the need for a sharp branch angle. Furthermore, it would be very difficult to create such a sharp branch angle using the UV direct

writing method since no mask would be used.

Here, a new Y branch consisting two standard arcs was numerically calculated and studied under the beam propagation method (BPM), with $\lambda = 1.31 \mu\text{m}$, background index of 1.45, and delta of 0.025. Figure 1(a) shows a basic structure with two output arms a and b; the main parameters are the radius of the curves R and the corresponding central angle β . It is clear that for as long as angle β remains relatively small (several degrees in Y branch application), a change in its value would have little impact on the branch output. The relationship between radius R and the output was studied for different waveguide widths. We set β as 6° and L as $350 \mu\text{m}$. Three waveguide widths (62.5 , 90 , and $120 \mu\text{m}$) were chosen for the output calculation. Only outputs of the upper branch were monitored in order to make the result simple and clear.

The result is illustrated in Fig. 1(b), with the variable scanning increment being $2000 \mu\text{m}$. The input power cannot be evenly divided simply by a random symmetric Y branch. Although there seems to be no regular pattern for the arm outputs, there are still certain R values at which the two outputs are almost the same for every simulation carried out. In these situations, the branch structure would be a 3-dB multimode power divider. Results show that in such simulation conditions with splitting ratio of 0.5 ± 0.01 , the values of the optimal arm radius are about 25.9 mm for the width of $62.5 \mu\text{m}$, 19.1 and 31 mm for $90 \mu\text{m}$, and a range from 40 to 45 mm for waveguide of $120 \mu\text{m}$ for an even power splitting. These results indicate that a larger waveguide width requires a wider optimal radius. In addition, the exact R value could be obtained by further analysis with smaller scan steps.

The straight Y branch has also been analyzed through comparison, which is shown in Fig. 1(c). The key parameter of this structure is the branch angle α , and the relationship between its value and the branch output has also been studied in the same way as the above, with the results given in Fig. 1(d). The figure illustrates that as α increases, the arm output drops rapidly, caused by the light leakage at the branch area in the case of big

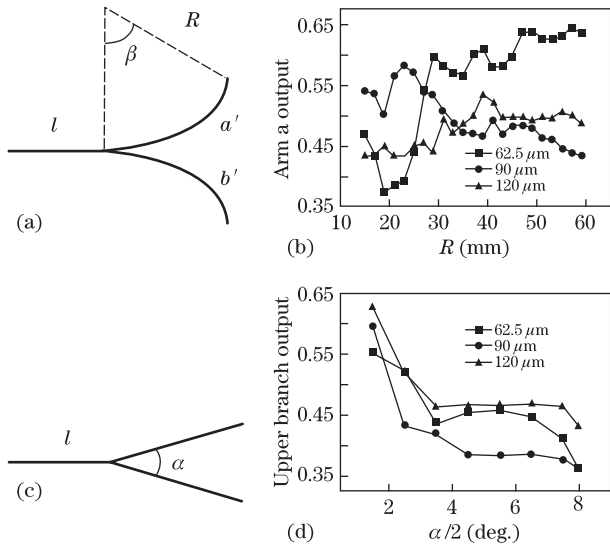


Fig. 1. (a) Scheme of multimode Y branch with curve arms; (b) arm output versus arm radius; (c) Y branch with straight arms; (d) upper branch output versus half branch angle.

angles. In order to achieve a good split ratio, the branch angle should be restricted to a very small one. It can be said that the Y branch in curves will offer more freedom in the splitter design than the one in straight lines; this will also make the fabrication through UV direct writing much more convenient as curves are easier to obtain than slashes.

In order to further divide the half light power and get one-fourth output, another cascaded splitting section must be added. Here, a unique branch structure is required to reach this goal, the asymmetric Y branch. This proposed design is based on a great number of trials in both simulation and fabrication. An asymmetric Y branch clearly offers more degrees of freedom required for a stable multimode power division than a symmetric one; therefore, finding the simplest configuration with few variables is the focus of this study. As shown in Fig. 2(a), the new branch is based on arm k and includes two arcs, m and n . We restrict our considerations in two cases: a) arm k is branched by m of the same radius and n with a radius that is to be determined; b) parameters for n and the position Q are pre-set, but the radius of m must be calculated. In either case, n is tangent to k at Q . Since the parameters for the first Y branch have already been studied and R already has a known value (25.95 mm in the case of $62.5 \mu\text{m}$ waveguide width), the starting angle of n is γ and the ending angle would be zero. Meanwhile, for curve m , the starting angle is also γ and its travel angle can be of any value that causes little output vibration, but it will eventually have an impact on the horizontal separation among the output ports.

For the purpose of making the case simple, we take situation a) with all the parameters settled except for the angle γ and the whole structure depends on the Q position and the radius of n . A situation analysis is conducted using a few values for the radii of n (25, 30, and 35 mm), and the output from arm n is simulated as a function of angle γ , as shown in Fig. 2(b). The result displays a periodic change in the split ratio; for each radius, there are a few angles of γ falling in the scan range at

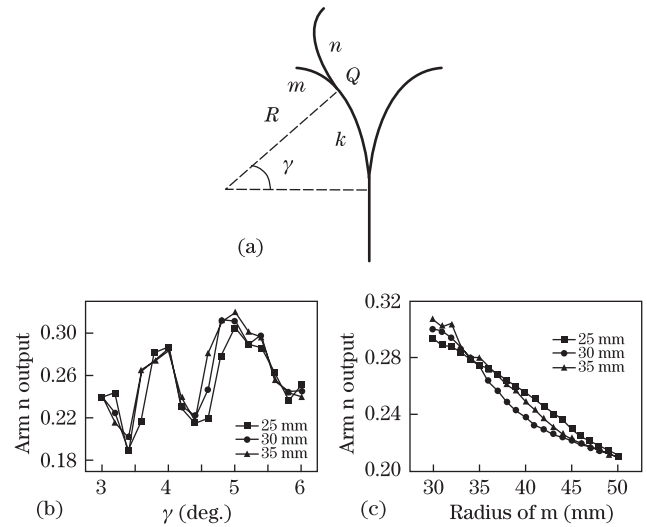


Fig. 2. (a) Structure of asymmetric secondary splitting branch; (b) arm n output versus γ with different radii; (c) arm n output versus radius m with γ to be 5° .

which the output ratio of 0.25 is reached. Interestingly, outputs at such radius are of the same trend, indicating a consistency in simulation. For case b), the value of γ and the parameters for n were pre-set by using some values that were practical in the fabrication process: $\gamma = 5^\circ$ and trial radii of n of 25, 30, and 35 mm. The result of the analysis is given in Fig. 2(c). It can be seen from the results that in this situation, the output of arm n decreases with increasing radius of curve m for the three selected radii of n . Furthermore, a relative smooth power dependence on the radius of m is observed for all the radii, which is very valuable in the design of multimode power splitters where instability of mode distribution is a main problem, even with a mode scrambler. Based on the abovementioned calculations, we believe that power splitting into four equal parts is feasible by using this configuration of secondary asymmetric Y branch.

The construction of a 1×4 device is described in details as follows. The components of the device are shown in Fig. 3(a). The view is rotated clockwise from Fig. 2. The construction of the device and the alignment of the output ports are taken into account simultaneously. The elements described in the figure include four arc curves (a , b , c , and d , with corresponding radii being R_1 , R_2 , R_3 , and R_4) and three straight lines connected with a , b , and d separately. Each of the curves is tangent to the one adjacent to it. The turning angle of c is denoted to be Δ . The ending angle is $\theta + \Delta$; the turning angle for d would be the same. The relationship between c and d is displayed in Fig. 3(b). We then have the following:

$$H_1 = R_3[\cos \theta - \cos(\theta + \Delta)] + R_4[1 - \cos(\theta + \Delta)] - R_2(1 - \cos \theta), \quad (1)$$

$$H_2 = (R_1 + R_2)(1 - \cos \theta). \quad (2)$$

In a properly designed splitter, there should be $H_1 = 2H_2$. Meanwhile, for the overall length L of the device, we yield

$$L = L_1 + L_2 + L_3 + L_4. \quad (3)$$

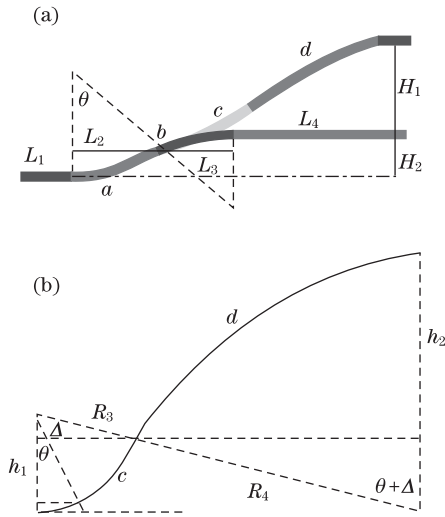


Fig. 3. (a) Components of the proposed 1×4 splitter (half of the structure is shown); (b) the geometric relationship between curves c and d .

This can be illustrated as

$$L = L_1 + (R_1 + R_2) \sin \theta + L_4. \quad (4)$$

For the formation of high-port devices, a tertiary asymmetric splitting branch will be needed to divide in half the one-fourth output and the same rules described above shall apply. For each type of divider, there are a few sets of parameters which would meet the output requirement, depending on the allowable overall length and output terminal separation.

The design procedure of 1×4 splitter would be very simple and can be described as follows. For a certain waveguide width, we pick the calculated value R_1 . For a given separation distance between adjacent ports, we pre-set θ and then calculate R_2 ; with a proper Δ value, we can get the value of R_4 .

A 1×4 multimode splitter at a waveguide width of $62.5 \mu\text{m}$ with port spacing of $400 \mu\text{m}$ was designed at first based on the abovementioned structural analysis and architecture principle. We chose a radius value for the first branch through calculation and then for the position of Q as introduced before. The remaining parameters were also made certain in this manner. The parameters for the splitter components are illustrated in Fig. 4 (half of the device is displayed for simplicity). The output results of the two ports were studied using these values, and they were given in Figs. 4(a) and (c).

The same designing rules were used for the formation of a 1×8 divider with a waveguide width of $120 \mu\text{m}$. Based on our research, another two asymmetric branches made of arc curves would be added to the branch arms of the one-fourth outputs. The structure parameters can also be determined using the abovementioned elemental principles. Half of the eight-port structure and the output results are shown in Figs. 4(b) and (d). The calculated results show that both splitters have excellent output performances.

Laser direct writing does not need mask and can reduce the device production procedure to minutes or even seconds. Figure 5 gives a schematic of the system setup for polymeric waveguide fabrication.

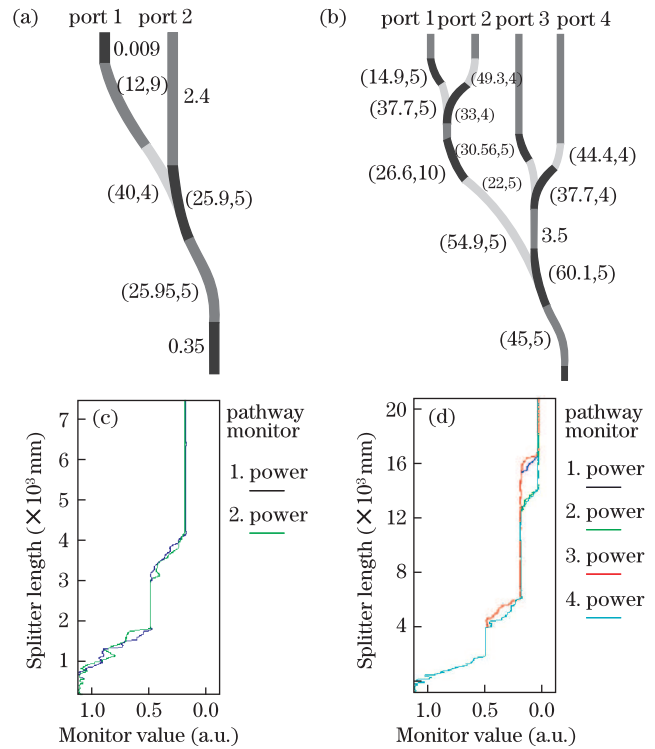


Fig. 4. (a) Half 1×4 divider structure and (c) the corresponding ports output; (b) half 1×8 divider structure and (d) the corresponding ports output. Labels in the formation of (i, j) indicate the curve parameters, i (unit in mm) stands for the radius value, while j (unit in degree) means the travel angle. Other numbers (unit in mm) indicate length of the straight waveguide.

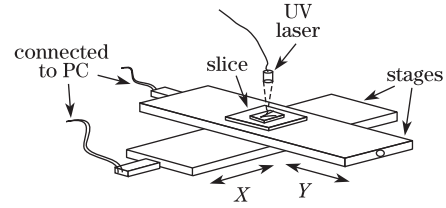


Fig. 5. Stages for laser direct writing of high movement accuracy.

The core part of the system is a two-dimensional translation stage (moving directions indicated by X and Y) of high motion accuracy controlled by PCI board C-843 installed in personal computer (PC) with a movement resolution of $0.1 \mu\text{m}$, which is commercially available from Physik Instrumente, Germany. The substrate for deposition is located on the top of the translation stage, and focused UV laser beam is irradiated onto the prepolymer coated on the substrate. The translation stage is capable of moving two perpendicular directions simultaneously to form various patterns. Meanwhile, the width of the waveguide is determined by the size of the UV beam spot.

A layer of optical-sensitive polymer (DeSolite[®] optical fiber coating, DSM Desotech) is spin-coated onto the surface of a microscope slide, which serves as a substrate, and is thoroughly cleaned beforehand. The thickness of the deposition is controlled to be $62.5 \mu\text{m}$ for 1×4 splitter and $120 \mu\text{m}$ for the eight-port device. Afterwards, the slide is placed onto the top of the upper stage. The

two stages are guided into movement by a pre-loaded program in the controlling PC, while the slide is being irradiated at the same time by laser light ($\lambda = 488 \text{ nm}$; light power of 40 mW; the light spot diameter could be varied between tens and hundreds of micrometers to achieve the desired waveguide width and control the light on and off status during the writing) from the above.

For straight waveguide writing, the stages move at a constant speed of $300 \mu\text{m/s}$, whereas for curvatures, certain acceleration and deceleration factors are needed for a variable motion to obtain smooth waveguide lines. When the writing process is done, further treatment is needed for the slide. Since the polymer has been partially cured by the UV laser beam, the unexposed part should be removed to develop the pattern. Conventional wet developing method is usually used; however, here, a particular treatment method based on air cleaning has been applied as a tool. We removed more than 90% of the unwanted polymer using a custom-sized compressed air knife edge with a width of 10 mm. The slide is then dripped with a few drops of ethanol and cleaned again using an air knife to reach total cleanness, leaving only the waveguide structure on the surface. This special dry method can reduce the usage of chemical solutions and enable high efficiency. To completely solidify the waveguide pattern for future handling, we put the slide into an UV oven (355 nm; power of 3 W), where the splitter is hardened by the more powerful UV irradiation for 3 min to reach a stable refractive index of 1.475.

The splitters fabricated by this means are shown in Fig. 6(a) as digital camera images. The total device length is 7.6 mm for the 1×4 splitter and 2.17 cm for the eight-port device. Figures 6(c) and (d) provide a close view of the output ports and the branching area for the splitter that is fabricated.

To evaluate the characteristics of the splitter, laser source with a wavelength of $1.31 \mu\text{m}$ was coupled into the input port by a $62.5\text{-}\mu\text{m}$ -diameter multimode fiber after both the input and output ports were cleaved. A CCD camera interfaced to the data acquisition software was used to obtain the output power distribution among the terminal ports. Figure 7 shows the outputs of the two splitters and their relative intensity. It can be seen in the left chart that the input power to the 1×4 device has been well divided into four parts. The power peak difference among them is less than 1%. Meanwhile, for the 1×8 divider, the maximum peak-to-peak difference is around 4%. Thus, it can be said that the four-port device has better performance compared with the eight-port device. Moreover, the average insertion loss for each

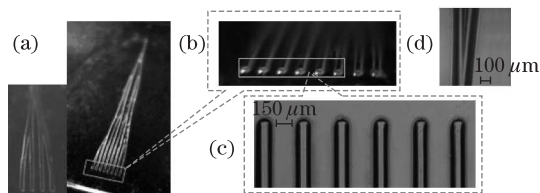


Fig. 6. (a) Splitters written by UV direct writing; (b) alignment of output ports; (c) enlarged top view of the output ports; (d) asymmetric Y branch.

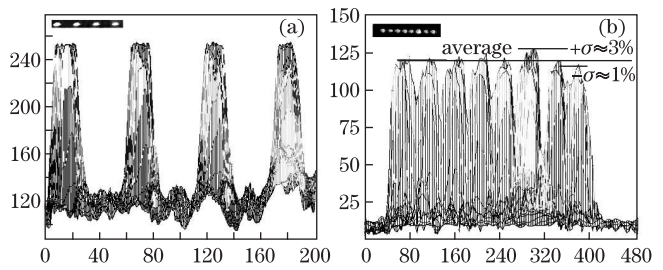


Fig. 7. Port outputs for (a) 1×4 and (b) 1×8 splitters.

output port was 8.6 dB for the 1×4 divider and 12.3 dB for the 1×8 divider. The additional loss is mainly due to the sidewall defects on the waveguides caused by the writing process, and these imperfections result in leakage in the total internal reflection process.

In conclusion, a design of multimode optical power splitter with asymmetric branches is proposed with a unique design principle. Two splitters with four and eight output ports are fabricated through UV direct writing. The splitter output uniformity is analyzed experimentally, and results prove that the device obtained by this approach has good performance for power splitting. This device may find applications in short-range high-speed data communications such as intra-board or inter-board data transmission. In addition, the fabrication method introduced in this letter can shorten the whole process down to 6–7 min.

References

1. T. F. Krauss, *Phys. Stat. Sol. (a)* **197**, 688 (2003).
2. S. Balslev, B. Bilenberg, D. Nilsson, A. M. Jorgensen, A. Kristensen, O. Geschke, J. P. Kutter, K. B. Mogensen, and D. Snakenborg, *Proc. SPIE* **5730**, 211 (2005).
3. L. Eldada and L. W. Shacklette, *IEEE J. Sel. Topics Quant. Electron.* **6**, 54 (2000).
4. W. Ni, X. Wu, and J. Wu, *Opt. Express*. **17**, 1194 (2009).
5. H. Lin, J. Su, R. Cheng, and W. Wang, *IEEE J. Quantum Electron.* **35**, 1092 (1999).
6. C. Huang, C. Chang, and W. Wang, *Microwave Opt. Technol. Lett.* **38**, 337 (2003).
7. J. Zhou, H. Shen, H. Zhang, and X. Liu, *Chin. Opt. Lett.* **7**, 1041 (2009).
8. Y. Gao, Z. Gong, R. Bai, Y. Hao, X. Li, X. Jiang, M. Wang, J. Pan, and J. Yang, *Chin. Phys. Lett.* **25**, 2912 (2008).
9. A. K. Das, *Appl. Opt.* **42**, 1236 (2003).
10. M. Olivero, M. Svalgaard, L. Jocou, and J. Berger, *J. Lightwave Technol.* **25**, 367 (2007).
11. K. Færch and M. Svalgaard, *IEEE Photon. Technol. Lett.* **14**, 173 (2002).
12. C. Peucheret, Y. Geng, M. Svalgaard, B. Zsigri, H. R. Sørensen, N. Chi, H. Deyerl, M. Kristensen, and P. Jeppesen, *IEEE Photon. Technol. Lett.* **17**, 1674 (2005).
13. M. Svalgaard, K. Færch, and L. Andersen, *IEEE Photon. Technol. Lett.* **21**, 2097 (2003).
14. S. Li, Q. Lin, W. Ni, X. Lou, and X. Wu, *Acta Opt. Sin. (in Chinese)* **28**, 1062 (2008).